The HIV Integrase Inhibitor Raltegravir Inhibits Felid Alphaherpesvirus 1 Replication by Targeting both DNA Replication and Late Gene Expression

Matthew R. Pennington,[a] Ian E. H. Voorhees,[a] Heather M. Callaway,[a] Shannon D. Dehghanpir,[b] Joel D. Baines,[b] Colin R. Parrish,[a] Gerlinde R. Van de Walle[a]

aBaker Institute for Animal Health, College of Veterinary Medicine, Cornell University, Ithaca, New York, USA
bDepartment of Pathobiological Sciences, School of Veterinary Medicine, Louisiana State University, Baton Rouge, Louisiana, USA

ABSTRACT Alphaherpesvirus-associated ocular infections in humans caused by human alphaherpesvirus 1 (HHV-1) remain challenging to treat due to the frequency of drug application required and the potential for the selection of drug-resistant viruses. Repurposing on-the-market drugs is a viable strategy to accelerate the pace of drug development. It has been reported that the human immunodeficiency virus (HIV) integrase inhibitor raltegravir inhibits HHV-1 replication by targeting the DNA polymerase accessory factor and limits terminase-mediated genome cleavage of human betaherpesvirus 5 (HHV-5). We have previously shown, both *in vitro* and *in vivo*, that raltegravir can also inhibit the replication of felid alphaherpesvirus 1 (FeHV-1), a common ocular pathogen of cats with a pathogenesis similar to that of HHV-1 ocular disease. In contrast to what was reported for HHV-1, we were unable to select for a raltegravir-resistant FeHV-1 strain in order to define any basis for drug action. A candidate-based approach to explore the mode of action of raltegravir against FeHV-1 showed that raltegravir did not impact FeHV-1 terminase function, as described for HHV-5. Instead, raltegravir inhibited DNA replication, similarly to HHV-1, but by targeting the initiation of viral DNA replication rather than elongation. In addition, we found that raltegravir specifically repressed late gene expression independently of DNA replication, and both activities are consistent with inhibition of ICP8. Taken together, these results suggest that raltegravir could be a valuable therapeutic agent against herpesviruses.

IMPORTANCE The rise of drug-resistant herpesviruses is a longstanding concern, particularly among immunocompromised patients. Therefore, therapies targeting viral proteins other than the DNA polymerase that may be less likely to lead to drug-resistant viruses are urgently needed. Using FeHV-1, an alphaherpesvirus closely related to HHV-1 that similarly causes ocular herpes in its natural host, we found that the HIV integrase inhibitor raltegravir targets different stages of the virus life cycle beyond DNA replication and that it does so without developing drug resistance under the conditions tested. This shows that the drug could provide a viable strategy for the treatment of herpesvirus infections.

KEYWORDS FeHV-1, raltegravir, terminase, ICP8, late gene expression, DNA replication, feline herpesvirus

Alphaherpesviruses are large DNA viruses that cause acute infection of mucosal and epithelial surfaces and that typically establish lifelong latency in neurons. These ubiquitous viruses cause a variety of diseases in many species (1). Human alphaherpesvirus 1 (HHV-1) (also known as herpes simplex virus 1) and human alphaherpesvirus 2 (HHV-2) (also known as herpes simplex virus 2) are highly prevalent and are associated with cold sores and genital ulceration, respectively (2). In addition, HHV-1 is

Address correspondence to Gerlinde R. Van de Walle, grv23@cornell.edu.

associated with chronic and recurrent ocular disease, characterized by conjunctivitis, corneal ulceration, and epithelial and stromal keratitis, often leading to corneal scarring and loss of transparency (3). All currently approved therapies for ophthalmologic alphaherpesvirus infection rely on nucleoside analogues that prevent base pairing when incorporated into the growing DNA polymer, thus inhibiting genome replication (4). However, and despite the proven value of these drugs in limiting HHV-1-associated corneal damage, effective treatment of this condition remains challenging due to toxicity concerns, the frequency of treatment required, and the potential for selection of drug-resistant variants, especially in immunocompromised individuals (5–8). Furthermore, it has been noted that a small percentage of patients with recurrent ocular herpes do not respond to treatment for unknown reasons (9). These factors may lead to high recurrence rates, resulting in damage to the ocular tissues that may progress to blindness.

Compared with the challenges of bringing a new drug to market, repurposing approved drugs to treat new conditions can accelerate the drug development process and reduce associated costs, since the safety and pharmacokinetic profiles of the drugs are already known (10, 11). This strategy has been used to identify approved therapeutics that, in addition to their on-label use, inhibit viral infection caused by ebolavirus, coronaviruses, and chikungunya virus (12–14). Raltegravir was approved by the U.S. Food and Drug Administration in 2007 for the treatment of human immunodeficiency virus (HIV) infection and functions as an integrase inhibitor (15). It specifically binds to an aspartic acid-aspartic acid-glutamic acid (DDE) motif located in the catalytic core domain of HIV integrase to prevent the strand transfer reaction that joins the 3′-processed viral cDNA ends to the host genomic DNA (gDNA), thus preventing integration (16, 17). The region targeted is structurally homologous to the RNase H domain of eukaryotic recombinases and transposases.

Two studies have explored the potential of using raltegravir as a novel antiherpesvirus therapy. The terminase protein (pUL89) of human betaherpesvirus 5 (HHV-5) (also known as human cytomegalovirus) contains an RNase H-like fold that is structurally similar, including containing a homologous DDE domain, to that of HIV integrase (18). Terminase is highly conserved across the herpesviruses and is responsible for cleaving newly synthesized concatemeric DNA into individual genome segments so that it can be packaged into assembling nucleocapsids. Consequently, herpesviral terminase has been previously proposed as a target for rational drug design, and the HHV-5 terminase inhibitor letermovir was recently approved by the U.S. Food and Drug Administration (19, 20). Raltegravir was shown to inhibit the nuclease function of HHV-5 pUL89 in an *in vitro* plasmid cleavage assay, suggesting it could function by preventing genome cleavage (18). Another group showed that raltegravir could also inhibit replication of HHV-1, but they mapped its activity to UL42, the DNA polymerase accessory factor, by sequencing a raltegravir-resistant HHV-1 strain (21). This suggests that raltegravir might be a useful drug for treatment of herpesvirus infection but that it may function differently depending on the *in vitro* assay used to evaluate functionality and/or the target herpesvirus family or species.

Felid alphaherpesvirus 1 (FeHV-1) causes ocular infections in cats, and due to the analogous presentations of the diseases in humans and cats, FeHV-1 is increasingly considered to be a useful natural-host model of ocular alphaherpesvirus infection (22, 23). Like HHV-1, FeHV-1 has similar challenges for successful treatment (24, 25). Our laboratory has shown previously that raltegravir can inhibit replication of FeHV-1, both in cell culture and in an *ex vivo* corneal explant model, comparably to the currently utilized antivirals (26). Furthermore, we recently demonstrated that raltegravir reduces FeHV-1 shedding duration and improves clinical outcomes in experimentally infected cats (C. B. Spertus, M. R. Pennington, G. R. Van de Walle, Z. I. Badanes, B. E. Judd, H. O. Mohammed, and E. C. Ledbetter, submitted for publication).

The goal of this study was to evaluate the mode of action of raltegravir against FeHV-1. In contrast to HHV-1, we were unable to select for a raltegravir-resistant FeHV-1 for sequencing purposes. We, therefore, used a candidate-based approach guided by
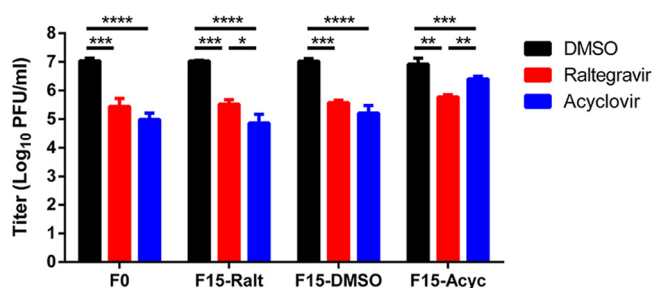
FIG 1 Generation of mutant FeHV-1 under continuous drug treatment. Wild-type (F0) FeHV-1 was passaged for 15 passages in the presence of increasing concentrations of raltegravir (F15-Ralt), DMSO (F15-DMSO), or acyclovir (F15-Acyc) and plaque purified. Drug susceptibility was assessed by infecting CRFK cells with the viruses at an MOI of 0.01 for 2 h. The inoculum was removed, and the cells were rinsed with low-pH citrate buffer. Growth medium containing DMSO, 500 μM raltegravir, or 160 μM acyclovir was then added. Cells and supernatants were collected together at 48 hpi, and viral titers were determined by plaque assay on CRFK cells. Significance for each virus was assessed by one-way ANOVA, with Tukey's HSD *post hoc* test. *, $P \leq 0.05$; **, $P < 0.01$; ***, $P < 0.001$; ****, $P < 0.0001$. The error bars indicate standard deviations.

the existing literature. We found that raltegravir did not impact FeHV-1 terminase function, as described for HHV-5, but instead targeted both DNA replication initiation and late gene expression, a mechanism consistent with inhibition of the functions of the early protein ICP8. Altogether, this work demonstrates that raltegravir targets multiple stages of the FeHV-1 life cycle and does so without developing drug resistance under the conditions tested.

RESULTS

FeHV-1 did not develop raltegravir resistance *in vitro*. A standard, unbiased approach to identify targets of antiviral drugs, and the one adopted by Zhou et al. (21) in the context of raltegravir and HHV-1, is to select for drug resistance, deep sequence the resultant virus, and then identify mutations associated with the drug resistance. We used a similar methodology to select for a raltegravir-resistant FeHV-1 strain by culturing the virus in increasing concentrations of raltegravir for 15 passages (F15-Ralt). The growth of both the original wild-type FH2CS strain of FeHV-1 (F0) and the F15-Ralt virus was reduced by approximately 1.5 $\log_{10}$ units following raltegravir treatment (Fig. 1), indicating that no resistant virus was selected. As expected, we observed no loss of raltegravir susceptibility by repeated passage of the virus in dimethyl sulfoxide (DMSO) (F15-DMSO) as a vehicle control (Fig. 1). To confirm that our methodology was appropriate, we selected for acyclovir resistance (F15-Acyc) as a positive control. We found that growth of the F0 virus was reduced by approximately 2.1 $\log_{10}$, units while growth of the F15-Acyc FeHV-1 was reduced by only 3-fold (Fig. 1). Furthermore, no significant differences in baseline growth between the F0, F15-DMSO, F15-Acyc, and F15-Ralt viruses were noted (one-way analysis of variance [ANOVA]; $P = 0.65$). Therefore, although our method was adequate to produce viruses resistant to nucleoside analogues, it did not select for raltegravir resistance, which is in contrast to what was found for HHV-1 (21).

Nevertheless, we decided to sequence the F0, F15-Ralt, and F15-Acyc viruses to determine if any single nucleotide polymorphisms (SNPs) resulted from extended passage in the presence of the antivirals. The F0 FH2CS strain exhibited 0.03% sequence divergence in protein-coding genes with the C-27 reference strain available in the National Center for Biotechnology Information (NCBI) database (NC_013590.2), in close agreement with the observed low genetic diversity of FeHV-1 isolates (27–29). Only 9 SNPs were detected in protein-coding genes, 6 conferring synonymous mutations (data not shown) and 3 conferring nonsynonymous mutations, all of which have been previously identified in other FeHV-1 isolates (Table 1). Extended passage in the presence of raltegravir did not produce any nonsynonymous mutations (Table 1), consistent with the absence of selection of a raltegravir-resistant virus. More specifi-

**TABLE 1** Nonsynonymous mutations in protein-coding genes associated with drug selection of FeHV-1[a]

Gene	Protein	Nucleotide mutation	Amino acid mutation
F0 vs C-27 reference strain			
UL29	ICP8 (ssDNA binding protein)	T3265C	S1089P
UL35	Minor capsid protein	T9G	S3R
US7	Glycoprotein I	T494C	M165T
F0 vs F15-Ralt			
None identified	None identified	None identified	None identified
F0 vs F15-Acyc			
UL30	DNA polymerase	T2167C	F723L

[a]Wild-type FH2CS strain FeHV-1 (F0), raltegravir-passaged (F15-Ralt), and acyclovir-passaged (F15-Acyc) viruses were sequenced on the Illumina platform. F0 was aligned with the FeHV-1 strain C-27 reference genome (NC_013590.2), and the drug-passaged viruses (F15) were aligned with F0 to identify amino acid changes in protein-coding genes.

cally, no mutations were identified in UL42, as had been described previously for raltegravir-resistant HHV-1 (21), or in the FeHV-1 terminase (UL15), as proposed for HHV-5 (18). In contrast, passage with acyclovir conferred a single amino acid mutation in UL30, the DNA polymerase (Table 1). While acyclovir resistance commonly maps to UL23, the viral thymidine kinase, HHV-1 acyclovir-resistant mutants mapping to UL30 have also been well described (30–32). These results further indicate that our methodology was appropriate for identification of drug resistance-associated SNPs for alphaherpesviruses. However, a more targeted approach was necessary to identify the mechanism, since FeHV-1 did not develop resistance to raltegravir.

Raltegravir partly inhibits viral DNA replication. As raltegravir had been reported previously to target UL42, the DNA polymerase accessory factor of HHV-1 (21), we decided to first explore the effects of raltegravir on FeHV-1 DNA replication using both single-step and multistep growth kinetics. During single-step replication kinetics, we observed an $\sim$1-$\log_{10}$-unit reduction in viral DNA replication with raltegravir therapy beginning as early as 4 h postinfection (hpi) (Fig. 2A, i). However, a slightly larger, $\sim$1.5-$\log_{10}$-unit reduction in the yield of progeny virus production was found (Fig. 2A, ii). Similarly, during multistep replication, we observed only an $\sim$0.5-$\log_{10}$-unit decrease in viral DNA replication following raltegravir treatment (Fig. 2B, i), but we observed a more substantial $\sim$3-$\log_{10}$-unit reduction in the production of fully infectious virus (Fig. 2B, ii). These results indicate that raltegravir does reduce viral DNA replication, similar to what was described for HHV-1 (21). However, the reduction in viral DNA synthesis was consistently smaller than the reduction in viral yields observed in both the single-step and multistep replication kinetics. We, therefore, hypothesized that raltegravir additionally targeted a second stage of the virus replication cycle, most likely downstream of viral DNA replication.

Raltegravir does not inhibit FeHV-1 genome packaging or terminase activity. Based on what was described previously for HHV-5 (18), we next evaluated whether raltegravir could block FeHV-1 terminase activity, using two experimental approaches. First, we performed electron microscopy to determine the effects of raltegravir on DNA packaging. This was based on a previous observation that inhibition of terminase activity with letermovir resulted in an accumulation of assembled HHV-5 capsids without DNA in infected cells, as observed by electron microscopy (33). Cells were infected with FeHV-1, treated with raltegravir 1 h later, and processed for electron microscopy at 7 hpi. We observed no difference in the number of capsids with versus without DNA (data not shown), indicating that viral terminase was most likely not affected. However, we did observe a statistically significant reduction in the total number of cells with viral capsids in raltegravir-treated infected cell cultures compared to DMSO-treated infected cell cultures (Fisher's exact test; $P = 0.023$) (Fig. 3A, i), as well
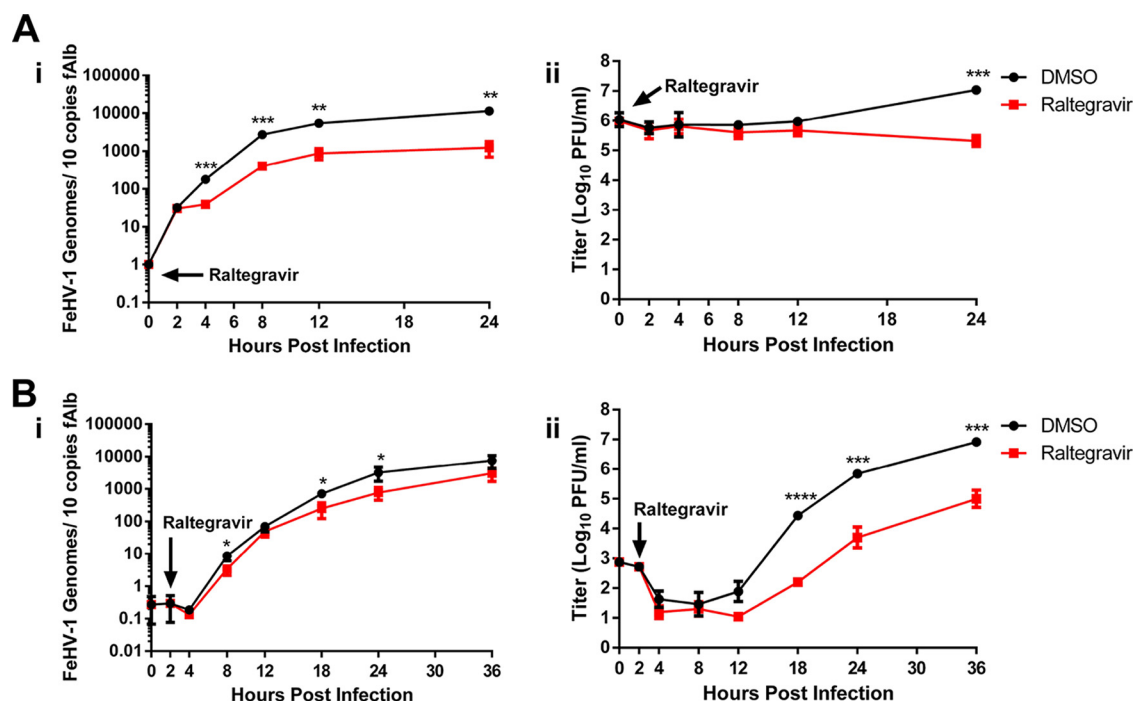
FIG 2 Growth kinetics of FeHV-1 following raltegravir treatment. (A) Single-step growth kinetics. CRFK cells were infected with FeHV-1 at an MOI of 10 and treated at the time of infection with DMSO or 500 μM raltegravir. (B) Multistep growth kinetics. CRFK cells were infected with FeHV-1 at an MOI of 0.01 for 2 h. The inoculum was removed, the cells were rinsed with low-pH citrate buffer, and media containing DMSO or 500 μM raltegravir was added. Cells and supernatants were individually collected at the indicated time points. Virus replication was assessed by qPCR of cellular samples (i) and titration of extracellular virus by plaque assay (ii). Student's t test; *, $P \leq 0.05$; **, $P < 0.01$; ***, $P < 0.001$; ****, $P < 0.0001$. The error bars indicate standard deviations.

as in the average number of capsids per nucleus (Student's t test; $P < 0.01$) (Fig. 3A, ii), indicating that raltegravir likely inhibits a stage at or before capsid assembly.

Second, we biochemically assessed the impact of raltegravir on viral terminase-mediated DNA cleavage. We expressed and purified the C-terminal nuclease-containing domain of the FeHV-1 terminase protein UL15 (pUL15-C). We then performed an *in vitro* nuclease activity assay, using the same protocol described for assessing HHV-1 termi-nase activity (34), in the presence or absence of raltegravir. When pUL15-C was mixed with a DNA plasmid, cleavage was observed, with the production of nicked and linearized products (Fig. 3B). When increasing concentrations of raltegravir were added, up to superphysiological concentrations of 10,000 μM, comparable amounts of DNA cleavage were still observed (Fig. 3B). As expected, (i) no cleaved DNA plasmid was observed in the absence of pUL15-C and (ii) plasmid DNA was fully linearized when treated with EcoRI (Fig. 3B). These results indicate that raltegravir does not inhibit FeHV-1 terminase-mediated genome cleavage, in contrast to what has been described for HHV-5 (18).

Raltegravir inhibits the early stages of DNA replication. It has previously been shown that XZ45, a hydrazide HIV integrase inhibitor that also targets the RNase H-like fold of integrase, can inhibit the replication of alpha-, beta-, and gammaherpesviruses (35). For HHV-1, this compound was proposed to target the early protein ICP8. ICP8 is a multifunctional viral protein essential for viral replication. It is required for DNA replication as a single-stranded DNA (ssDNA) binding protein and plays a role in the initiation of DNA replication in conjunction with the origin binding protein UL9 (36–40). It also has a separate role in the initiation of late gene expression (41, 42) and is thought to be important for viral recombination (43). Interestingly, ICP8 is also known to contain an RNase H-like domain homologous to that of HIV integrase (35). We therefore hypothesized that raltegravir could target FeHV-1 ICP8.

However, we first needed to address the observed point mutation in ICP8 of FH2CS, the FeHV-1 strain used in the present study, compared to that of the reference strain,
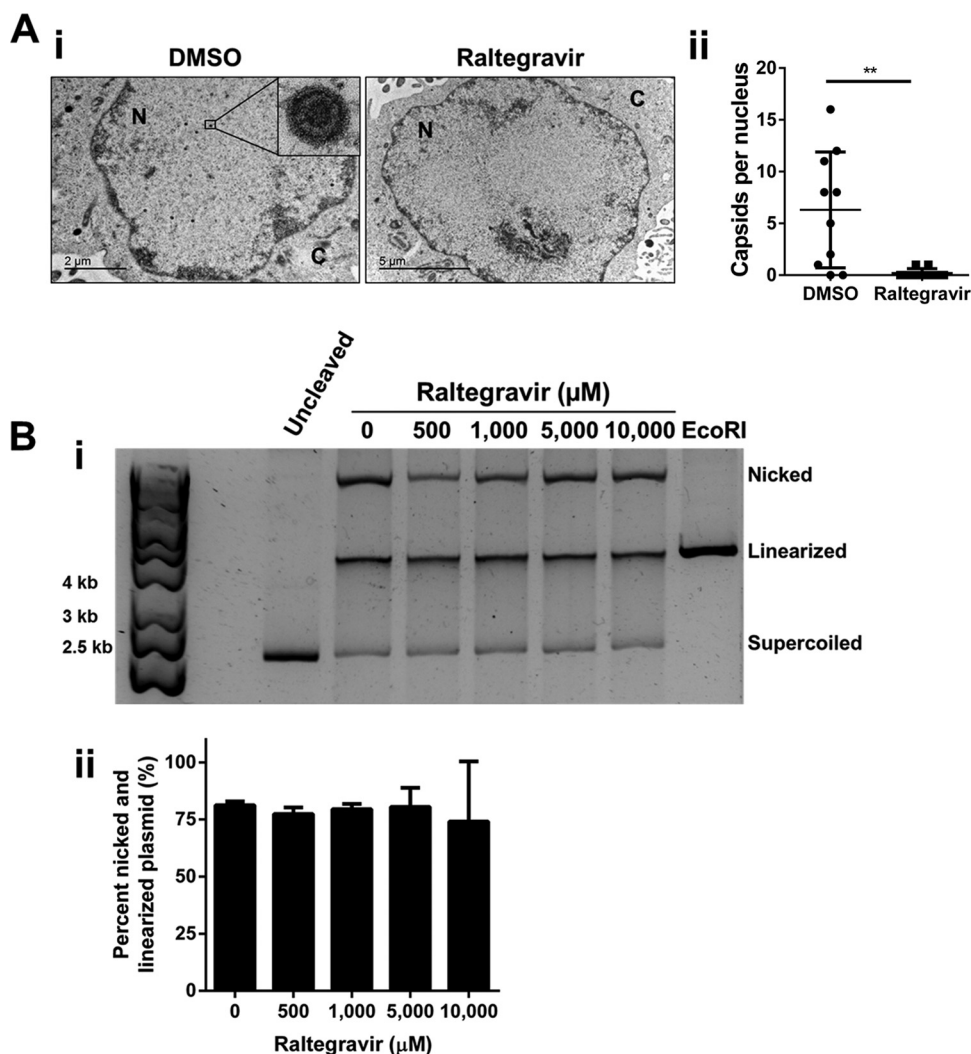
FIG 3 Raltegravir does not block terminase-mediated genome cleavage. (A) Electron microscopy. CRFK cells were infected with FeHV-1 at an MOI of 3 for 1 h, treated with DMSO or 1,000 μM raltegravir, and processed for imaging at 7 hpi. (i) Representative electron microscopy images assessing FeHV-1 capsid formation. The inset shows the morphology of the indicated nucleocapsid. N, nucleus; C, cytoplasm. (ii) Average numbers of capsids per nucleus. Student's t test; **, $P < 0.01$. (B) Biochemical assessment of terminase inhibition. Recombinant FeHV-1 pUL15-C was mixed with the pET-20b(+) plasmid and increasing concentrations of raltegravir. Uncleaved and EcoRI-cleaved plasmids were included as controls. Following digestion for 1 h at 37°C, the products were separated by agarose gel electrophoresis to identify plasmid cleavage. (i) Representative gel. (ii) Percentages of nicked and linearized plasmid. The error bars indicate standard deviations.

C-27 (Table 1). Crandell Rees feline kidney (CRFK) cells were infected with either virus strain and treated with raltegravir or DMSO as a vehicle control, and viral titers were determined by plaque assay. As determined by one-way ANOVA with Tukey's honestly significant difference (HSD) *post hoc* test, no difference in susceptibility to raltegravir was found between FH2CS and C-27. Furthermore, there were no differences in virus production at baseline levels between the strains, indicating that this mutation does not affect virus viability or drug susceptibility (Fig. 4).
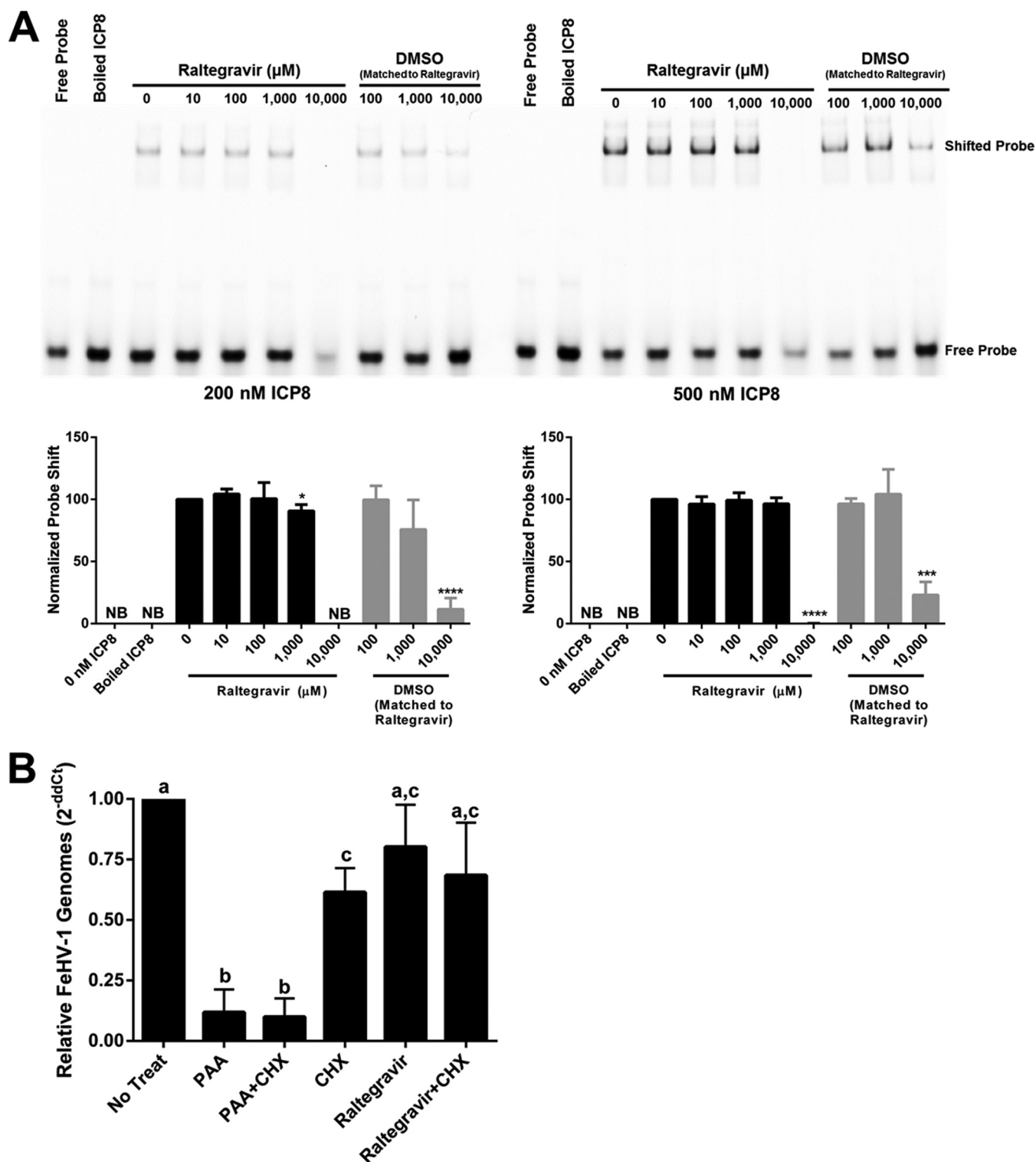
Raltegravir could inhibit DNA replication via ICP8 by interfering with its ability either to bind ssDNA or to initiate DNA synthesis. In order to test the effects of raltegravir on ICP8 ssDNA binding, we recombinantly expressed FeHV-1 ICP8. Utilizing an electromobility shift assay, we found that raltegravir did not interfere with ICP8's ability to bind ssDNA, except at high concentrations (Fig. 5A). We observed a similar reduction in ssDNA binding when a volume-matched amount of DMSO was added, indicating that this reduction is likely due to the effects of the vehicle, rather than the drug itself (Fig. 5A). These results indicate that raltegravir likely does not affect ICP8 ssDNA binding, in line with what has been reported previously for the activity of XZ45 against HHV-1 (35).
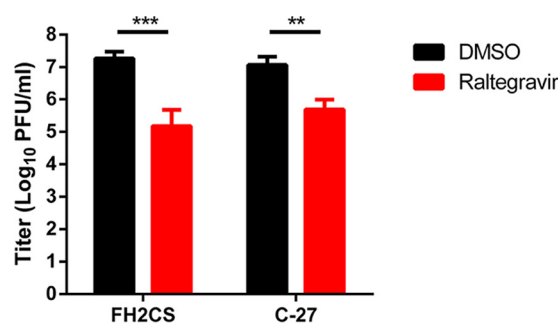
FIG 4 Raltegravir is similarly effective against the FeHV-1 strains FH2CS and C-27. CRFK cells were infected with FeHV-1 strain FH2CS or C-27 at an MOI of 0.01 for 2 h. The inoculum was removed, the cells were rinsed with low-pH citrate buffer, and medium containing DMSO or 500 μM raltegravir was added. Cells and supernatants were collected together at 48 hpi, and viral titers were determined by plaque assay on CRFK cells. Significance was assessed by one-way ANOVA, with Tukey's HSD *post hoc* test. **, $P < 0.01$; ***, $P < 0.001$. The error bars indicate standard deviations.

Next, we sought to determine if raltegravir inhibits the initiation of DNA replication, which requires ICP8. Since ICP8 is essential for viral replication, it is not possible to create viable mutant viruses deficient in the complete protein. We therefore adapted a previously described polymerase-pausing experiment (44) to address our question indirectly. Briefly, cells were infected and treated with a high dose of phosphonoacetic acid (PAA) for 12 h. Since PAA inhibits DNA replication via inhibition of the DNA polymerase, this results in the initiation of DNA replication, but not DNA elongation, thereby effectively "pausing" DNA synthesis at this stage (45). The PAA block was then released by washing away the drug. The following fresh drugs were then added: (i) PAA, to continue to inhibit DNA elongation; (ii) cycloheximide (CHX), to allow DNA elongation but not cellular or viral protein translation; (iii) raltegravir, to determine its effects; or (iv) a combination of these drugs (Fig. 5B). Genome replication was assessed by quantitative PCR (qPCR) for each of these conditions and normalized to that of cells that were left untreated after PAA removal in order to permit full viral replication. As expected, PAA continued to effectively inhibit genome synthesis when given both alone and in combination with CHX (Fig. 5B). CHX, in contrast, only minimally affected genome synthesis when given after DNA replication was initiated (Fig. 5B). Similarly, we found that raltegravir, both alone and in combination with CHX, did not affect genome replication (Fig. 5B). As raltegravir no longer inhibited genome replication following release of the PAA block, this indicates that it must impact DNA replication at an early stage, prior to DNA elongation. This is consistent with inhibition of ICP8 activity during the initiation of DNA synthesis and inconsistent with an effect on polymerase processivity, as was proposed previously for HHV-1.

Raltegravir specifically downregulates late gene expression, independently of DNA replication. In addition to its known roles in DNA replication, ICP8 also independently stimulates transcription of at least three late genes, the glycoprotein C (gC), glycoprotein D (gD), and UL47 genes (41, 42). To determine the effects of raltegravir on FeHV-1 gene expression, we adopted a methodology similar to that used to originally define the effects of ICP8 on late gene expression (41, 42). To this end, cells were infected at a high multiplicity of infection (MOI), treated with raltegravir, and collected at 6 hpi for quantitative reverse transcription (qRT)-PCR analysis. We observed an ~50% reduction in viral genome replication (Fig. 6A), which is similar to what we observed previously in the single-step growth kinetics (Fig. 2B, i). At this time point, we found that raltegravir had no effect or drove a slight upregulation of immediate-early genes (Fig. 6B), consistent with inhibition of viral DNA replication. We also observed no effect or only a slight downregulation of the two early genes that we tested, including the ICP8 gene itself. In contrast, we observed a significant downregulation of 7 out of the 9 late genes that we assessed, including the gC and gD genes (Fig. 6B). To determine if the downregulation of late genes was (i) a direct consequence of the reduction in

FIG 5 Raltegravir inhibits an early stage of DNA replication, consistent with ICP8 inhibition. (A) Raltegravir does not block ICP8 single-stranded-DNA binding activity. Recombinant FeHV-1 ICP8 (200 or 500 nM) was mixed with a Cy3-labeled ssDNA probe and increasing concentrations of raltegravir or volume-matched amounts of DMSO for 1 h at 37°C. ICP8-bound and unbound probes were resolved by native PAGE electrophoresis, and the percentage of shifted probe, normalized to the 0-μM raltegravir samples, was calculated. NB, no binding. Student's t test, comparing each concentration to 0 μM raltegravir; *, $P < 0.05$; ***, $P < 0.001$; ****, $P < 0.0001$. (B) Raltegravir inhibits an early stage of viral DNA replication. CRFK cells were infected with FeHV-1 at an MOI of 2 for 12 h and treated at the time of infection with 100 μg/ml PAA to allow the initiation of DNA replication, but not strand elongation. The inoculum and PAA were removed and replaced with cell line medium containing no drugs, 100 μg/ml PAA, 100 μg/ml PAA with 50 μg/ml CHX, 50 μg/ml CHX, 500 μM raltegravir, or 500 μM raltegravir with 50 μg/ml CHX. The cells were cultured for an additional 16 h, at which point they were collected and processed for relative genome replication using qPCR. Significantly different groups ($P < 0.05$), as determined by one-way ANOVA with Tukey's HSD *post hoc* test, are indicated using different letters. The error bars indicate standard deviations.
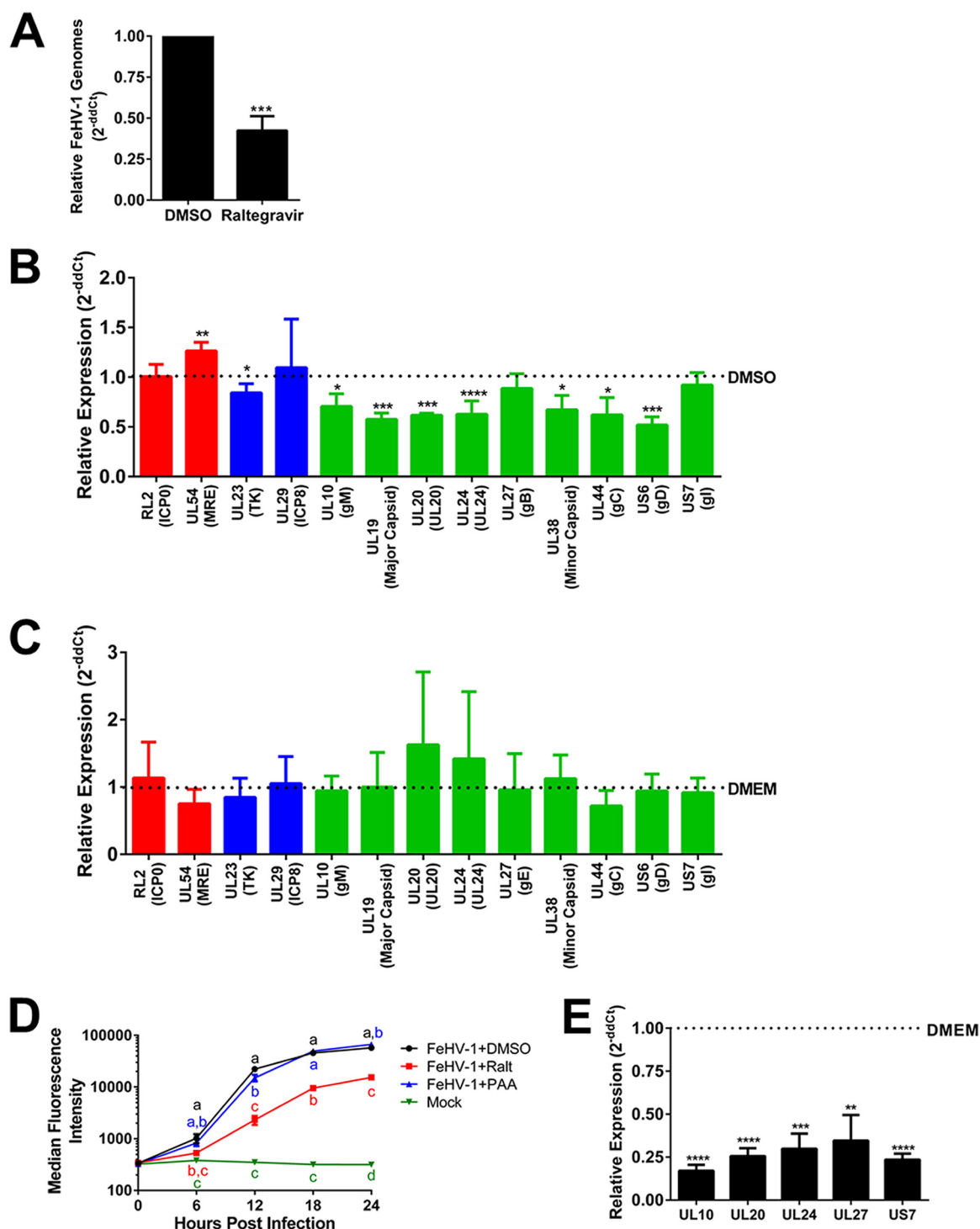
FIG 6 Raltegravir specifically inhibits late gene expression, consistent with ICP8 inhibition. Primary feline corneal epithelial cells (FCECs) were infected with FeHV-1 at an MOI of 10 and treated at infection with 500 μM raltegravir, 12.5 μg/ml PAA, or the indicated vehicle control. Cells were collected at 6 hpi for analysis. (A) Relative viral genomic DNA replication following raltegravir treatment, as determined by qPCR. (B and C) Relative expression of immediate-early (red), early (blue), and late (green) viral genes. Shown is relative gene expression, as determined by qRT-PCR, following raltegravir (B) and PAA (C) treatment. (D) Flow cytometric analysis of gD protein expression. FCECs were infected with FeHV-1– gD–DsRed at an MOI of 3 and treated at the time of infection with DMSO, 500 μM raltegravir, or 12.5 μg/ml PAA or left uninfected. At the indicated time points, cells were collected and analyzed by flow cytometry. Significantly different groups ($P < 0.05$), as determined by one-way ANOVA with Tukey's HSD *post hoc* test, are indicated using different letters. (E) Treatment with PAA inhibits late gene expression. FCECs were infected with FeHV-1 at an MOI of 10 and treated at the time of infection with 200 μg/ml PAA. Cells were collected at 6 hpi, RNA was isolated, and expression of select late genes relative to DMEM-treated controls was assessed by qRT-PCR. Student's *t* test; *, $P \leq 0.05$; **, $P < 0.01$; ***, $P < 0.001$; ****, $P < 0.0001$. The error bars indicate standard deviations.

DNA replication, as expression of late genes is known to be partially dependent on DNA replication (46), or (ii) an independent effect on late gene expression specifically, we repeated the experiment using PAA instead of raltegravir, an approach that was used previously to define the roles of ICP8 during HHV-1 replication (41, 42). When treating infected cells with PAA, using a concentration that we previously determined resulted in a level of inhibition of FeHV-1 genome replication similar to that of raltegravir (47), we did not observe downregulation of any of the tested genes (Fig. 6C). Next, we wanted to confirm this downregulation of late gene expression in raltegravir-treated FeHV-1-infected cells on the protein level. However, since monoclonal antibodies targeting single FeHV-1 proteins are not commercially available, we utilized a recombinant FeHV-1 strain expressing the DsRed Express2 fluorophore fused to the C terminus of glycoprotein D (FeHV-1–gD–DsRed) (48). The virus was suitable for these experiments, as gD expression was found to be downregulated by raltegravir, but not PAA, treatment (Fig. 6B and C). Similar to the mRNA expression results, we found gD protein expression to be reduced upon raltegravir treatment (Fig. 6D). In contrast, gD protein was produced at approximately the same rate in PAA-treated infected cells and DMSO-treated control cells (Fig. 6D). To confirm that PAA (i) can indeed result in reduced late gene expression upon reducing DNA replication and (ii) was functioning properly in our hands, we treated FeHV-1-infected cells with 200 μg/ml PAA, which previously was shown to inhibit FeHV-1 DNA replication by over 99% (47), and defined the expression of a subset of late genes. Using this dose, FeHV-1 late gene expression was decreased to approximately 25% of that of untreated controls (Fig. 6E), which is in close agreement with what has been described for HHV-1 treated with PAA (49). Collectively, while raltegravir also inhibited viral DNA replication, these results support a mechanism involving further specific inhibition of late gene expression by raltegravir. This appeared to proceed through a mechanism independent of the observed direct effect on inhibiting DNA replication, as treatment with a comparable dose of PAA did not inhibit late gene expression. This further supports a mechanism by which raltegravir inhibits known functions of ICP8.

DISCUSSION

The goal of the present study was to evaluate the mode of action of the HIV integrase inhibitor raltegravir against FeHV-1, an alphaherpesvirus closely related to HHV-1 that also causes severe ocular disease. In contrast to previous studies reporting that raltegravir inhibits terminase-mediated genome cleavage of HHV-5 (18) and DNA replication of HHV-1 via interference with the DNA polymerase accessory factor (21), we propose that raltegravir targets the ICP8 protein of FeHV-1, similar to the hydrazide-based integrase inhibitor XZ45 (35). Both ICP8 and HIV integrase belong to the DDE recombinase class of enzymes that coordinate divalent metal cations in their active sites within an RNase H-like fold (18, 50). Their shared domains, therefore, suggest a structural basis for an interaction between raltegravir and ICP8.

Functionally, ICP8 is required for viral replication and has at least four well-defined roles in the life cycle of alphaherpesviruses. The centrality of the protein in viral replication may explain why we were unable to select for raltegravir resistance. Indeed, it may be difficult to introduce mutations in such a vital protein without loss of functionality. First, ICP8 was originally identified as the primary ssDNA binding protein, binding in a non-sequence-specific manner to stabilize the open replication forks during DNA replication (36, 51). Similar to XZ45, we found that raltegravir did not inhibit the ability of ICP8 to bind ssDNA. Second, ICP8 has been shown to interact with and stimulate the helicase activity of UL9, the origin binding protein, to mediate the initiation of DNA replication (52). These proteins accumulate at the origins of replication on the viral DNA (53), and it is thought that ICP8 binds to an inhibitory region of UL9, thereby acting as a positive regulator to neutralize the region and increase the efficiency of the UL9-mediated DNA opening (54). Using a DNA polymerase-pausing assay (44), we observed that raltegravir specifically inhibited an early stage of DNA replication prior to processive DNA elongation mediated by the DNA polymerase and

its accessory factor. It is possible that this early-stage inhibition is due to raltegravir blocking the ability of ICP8 to either bind to or activate UL9 helicase activity, although additional experiments are needed to study this. Moreover, this result does not exclude the possibility that ICP8 impacts other proteins necessary for DNA replication initiation, including UL9, the helicase, and/or the primase. Third, it has been shown that ICP8 mediates the transcription of at least three late genes, the gC, gD, and UL47 genes, via a DNA replication-independent mechanism thought to involve interactions with other viral and host proteins (42). Consistent with this, we found that raltegravir treatment resulted in a reduction of many late genes, including both gC and gD gene transcripts, independently of DNA replication, and we confirmed this for gD on the protein level. Similar to our results, XZ45 was also shown to reduce gC protein expression in HHV-1-infected cells, consistent with inhibiting ICP8 function (35). Although it has not been determined which additional late genes may depend on ICP8, our results suggest that the gM, UL19, UL20, UL24, and UL38 genes may also be transcriptionally regulated either directly or indirectly by ICP8. Consistent with the known activity of ICP8 (42), raltegravir appeared to exhibit no preference for γ1 or γ2 genes, as both gD, a model γ1 gene (55), and gC, a model γ2 gene, were downregulated following treatment. Fourth, it has been shown that ICP8, either by itself or in combination with the UL12 exonuclease, can mediate strand invasion to promote homologous recombination (56, 57). It has been suggested that alphaherpesvirus DNA replication may involve a recombination-dependent replication stage due to the presence of genome concate-mers that form complex structures and inversion of the L and S genome segments (39). The precise mechanisms by which this relates to DNA replication remain poorly understood, although it has been proposed that the strand invasion activity mediates the transition from theta form replication to rolling-circle DNA synthesis (35, 58). While we did not investigate the effects of raltegravir on viral recombination during FeHV-1 infection, XZ45 was shown to inhibit HHV-1 recombination both *in vitro* and during viral coinfections (35). It is tempting, therefore, to speculate that raltegravir may also inhibit viral recombination, further leading to the observed inhibition of DNA replication.

For HHV-1, it was found that raltegravir resistance mapped to a V296I mutation in UL42, the DNA polymerase accessory factor (21). It was hypothesized that the drug might block the interaction of UL42 with other components of the replication complex (i.e., DNA polymerase, helicase, and primase) based on the position of the mutation in the protein. Raltegravir reduced by ~50% the gDNA replication of a recombinant HHV-1 bearing this UL42 mutation compared to an ~80% reduction with wild-type HHV-1. Based on this, the authors concluded that they were unable to exclude the possibility that additional viral proteins were affected by the drug, leaving open the possibility that raltegravir may also affect HHV-1 ICP8 function. Likewise, we cannot rule out some interference of raltegravir with the functions of FeHV-1 UL42, contributing in part to the observed inhibition of DNA replication in raltegravir-treated, FeHV-1-infected cells.

A screen of HIV RNase and integrase inhibitors revealed that synthetic α-hydroxytropolones are also effective against HHV-1 and HHV-2, further highlighting the value of and interest in using HIV inhibitors against herpesviruses (59). These compounds were also initially hypothesized to inhibit either ICP8 or the nuclease function of HHV-1 terminase, based on the structural homology of the proteins with the RNase H-like folds in HIV proteins (60). The effects of these compounds on HHV-1 ICP8 function were not explored. However, when their effects on HHV-1 pUL15-C-mediated DNA cleavage were investigated, it was found that the compounds that strongly inhibited HHV-1 replica-tion had little effect on pUL15-C activity *in vitro* (60). These results are consistent with our observation that raltegravir inhibited FeHV-1 replication without apparent effects on pUL15-C activity. It was also recently reported that these α-hydroxytropolones could inhibit the replication of a range of alphaherpesviruses, including FeHV-1 (61). They demonstrated that the compounds inhibited HHV-1 DNA replication rather than ge-nome cleavage, similar to our observations with raltegravir. Three proteins were noted to possess either RNase H-like domains or activity that the compounds could target to

account for these effects: UL30, the DNA polymerase; UL12, the alkaline nuclease; and ICP8. However, neither the effects of the compounds specifically on these proteins nor their effects on FeHV-1 DNA replication and protein expression were evaluated, leaving this an open question. Raltegravir, likewise, could have theoretically also impacted UL30 or UL12 function. However, our results from the DNA polymerase-pausing experiment (Fig. 5B) and gene expression results (Fig. 6A to C) are inconsistent with raltegravir affecting only UL30 and/or UL12 and are consistent with inhibition of the multiple functions of ICP8. Nevertheless, effects on the RNase H activity of UL30 and/or UL12, in addition to the effects on ICP8, cannot be excluded.

Taken together, this study adds to the body of literature that suggests that HIV integrase inhibitors can also be useful in the treatment of herpesvirus infections. More specifically, no approved inhibitors of ICP8 exist today, and to our knowledge, no inhibitors other than XZ45 with experimentally supported inhibitory activity against ICP8 are in development. As such, repurposing raltegravir to inhibit ICP8, either alone or in combination with traditional nucleoside analogues, may be a novel strategy to treat herpesvirus infections.

MATERIALS AND METHODS

Cells, viruses, and drugs. CRFK cells (American Type Culture Collection) were maintained in cell line medium consisting of Dulbecco's modified Eagle medium (DMEM) with 1 g/liter glucose, L-glutamine, and sodium pyruvate, supplemented with 10% fetal bovine serum and penicillin (200 U/ml)-streptomycin (200 μg/ml). Primary feline corneal epithelial cells (FCECs) were isolated from specific-pathogen-free cats euthanized for reasons unrelated to the current study and cultured as previously described (47, 62). Cell lines were maintained at 37°C and 5% CO_2. The FeHV-1 strain FH2CS (63) was used for all experiments and compared with the FeHV-1 strain C-27 (64) for sequencing and drug susceptibility purposes. For flow cytometry, a recombinant FH2CS FeHV-1 strain (FeHV-1–gD–DsRed) was used, which we generated in house using clustered regularly interspaced short palindromic repeat (CRISPR)/Cas9 genome engineering to express DsRed Express 2 fused to the C-terminal end of glycoprotein D (48). All viral stocks were grown and their titers were determined on CRFK cells, as previously described (26). Raltegravir (ChemieTek, Indianapolis, IN) and acyclovir (Sigma-Aldrich, St. Louis, MO) were diluted in DMSO. PAA and CHX (Sigma-Aldrich) were both diluted in DMEM. All the drugs were stored at −20°C until use.

Generation, validation, and deep sequencing of drug-resistant herpesviruses. Putative drug-resistant herpesviruses were generated as previously described for selection of a raltegravir-resistant HHV-1 strain (21). Briefly, confluent CRFK cells in T25 flasks (Grenier Bio-One, Monroe, NC) were infected with 300,000 PFU of FeHV-1 in the presence of 200 μM raltegravir, 80 μM acyclovir, or DMSO. Cells were collected by freeze-thawing three times and centrifuging at 300 $\times$ g for 5 min to remove cellular debris when robust cytopathic effect was apparent, typically 2 days postinfection. Then, 2 μl of the passaged cells was used to inoculate new CRFK cells in the same manner, and 7 passages were performed with these drug concentrations. Three passages were then performed in 500 μM raltegravir, 160 μM acyclovir, or DMSO. Virus stocks were plaque purified and selected for an additional 5 passages in 500 μM raltegravir, 160 μM acyclovir, or DMSO, and stocks of the 15th passage (F15) were prepared.

Drug resistance was evaluated by infecting confluent CRFK cell cultures with the wild type, designated F0; DMSO-passaged (F15-DMSO); raltegravir-passaged (F15-Ralt); or acyclovir-passaged (F15-Acyc) FeHV-1 at an MOI of 0.01 for 2 h at 37°C. The cultures were then rinsed with ice-cold, low-pH citrate buffer to reduce cell-associated virus, and growth medium supplemented with DMSO, 500 μM raltegravir, or 160 μM acyclovir was added. Cells and supernatants were collected at 48 hpi by freeze-thawing three times. The titers of samples on CRFK cells were determined as previously described (26). The susceptibility of the FH2CS strain versus the C-27 strain to 500 μM raltegravir was determined using the same method.

Plaque-purified herpesvirus isolates were deep sequenced as previously described (65). Briefly, confluent CRFK cells were infected with 2 μl of F0, F15-DMSO, F15-Ralt, or F15-Acyc FeHV-1. Cells were collected via trypsinization when a robust cytopathic effect was visible, approximately 2 days postinfection. Genomic DNA was isolated using a Qiagen blood and tissue kit (Qiagen, Valencia, CA). One nanogram of DNA, quantified using a Qubit DNA HS assay kit (Thermo-Fisher Scientific, Waltham, MA), was used for library preparation with a Nextera XT library prep kit (Illumina Inc., San Diego, CA) according to the manufacturer's protocol. Deep sequencing was performed on the MiSeq platform (Illumina, Inc.) with 250-nucleotide (nt) paired-end reads. Initial *de novo* assemblies, using SPAdes (version 3.9.0), did not produce full-length FeHV-1 genome sequences, and reads were subsequently mapped to the FeHV-1 C-27 reference genome (NC_013590.2) with Geneious (version 10.2.2; Biomatters Ltd., Auckland, New Zealand) using the default medium-low sensitivity settings. Reference mapping revealed that our sequencing approach failed to generate reads over the intergenic palindromic repeats and G/C-rich regions of the FeHV-1 genome. As these regions are noncoding and therefore were not expected to influence drug susceptibility phenotypes, they were excluded from our analysis. For each viral isolate, our sequencing completely captured all annotated protein-coding regions in the FeHV-1 genome, with an average coverage of >125. Majority consensus sequences were determined for all protein-coding

regions, and mutations differentiating the experimental treatment groups from control viruses were identified.

Viral growth kinetics. Viral growth kinetics were assessed by single-step and multistep growth curves. For single-step kinetics, confluent CRFK cells were infected with FeHV-1 at an MOI of 10 and treated with DMSO or 500 μM raltegravir at the time of infection. At designated time points, the medium was removed and centrifuged at 1,000 $\times$ g for 5 min to pellet cellular debris. Cells were collected via trypsinization and combined with the centrifuged cellular debris. Cell-free extracellular virus titers were determined using plaque assays (26). Genomic DNA was isolated from cellular samples using a Qiagen blood and tissue kit. Viral genome replication was determined using absolute qPCR, as previously described (Spertus et al., submitted). For multistep kinetics, confluent CRFK cells were infected with FeHV-1 at an MOI of 0.01 for 2 h. The inoculum was then removed, and residual extracellular virus was reduced by rinsing with low-pH citrate buffer. Growth medium containing DMSO or 500 μM raltegravir was added. Cells were collected at designated time points and processed as for the multistep kinetics curve.

Electron microscopy. Capsid formation was evaluated as previously described (66). Confluent CRFK cells were infected with FeHV-1 at an MOI of 3 for 1 h. The inoculum was removed and replaced with cell line medium containing DMSO or 1,000 μM raltegravir. At 7 hpi, the cells were fixed in fixative solution consisting of 2% formaldehyde and 2.5% glutaraldehyde in 0.1 M sodium phosphate buffer, pH 7.4, for 10 min at room temperature (RT). The cells were harvested by scraping, pelleted by centrifugation, resuspended in fixative solution, and incubated for 2 h at RT with shaking. The cells were pelleted by centrifugation; resuspended in an equal amount of 3% agarose; and, when solidified, cut into 1- to 2-mm cubes. The cubes were then placed in a glass vial of 0.1 M sodium phosphate buffer; washed 5 times, for 15 min each time, with 0.08 M glycine in 0.1 M sodium phosphate buffer; fixed in 2% OsO$_4$ in 0.1 M sodium phosphate buffer in the dark for 1 h; and then washed 3 times, for 5 min each time, in water. The cells were dehydrated through a series of increasing ethanol concentrations (50%, 70%, 80%, and 90% for 15 min each and 100% for 20 min; 3 times). After dehydration, the cells were infiltrated with 1:1 ethanol-LR white resin (Electron Microscopy Sciences, Hatfield, PA). One cell pellet was placed into the bottom of a Beem capsule (Electron Microscopy Sciences), covered in resin, and incubated for 24 h at 65°C. Ultrathin (90-nm) sections for transmission electron microscopy were cut on a Leica EM UC7 microtome. The sections were stained with 2% uranyl acetate for 5 min, followed by 2% lead citrate for 3 min, and 10 independent sections for each condition were photographed with a JEOL JEM-1400 transmission electron microscope.

FeHV-1 terminase expression, purification, and activity assay. The C-terminal nuclease-containing domain of UL15 (pUL15-C), from amino acid 477 to 735, approximately corresponding to what has previously been described for HHV-5 pUL89-C (18), was expressed in *Escherichia coli*. Briefly, this region of UL15 was cloned into the pET-His-TEV plasmid (a kind gift from Yuxin Mao, Cornell University) between the BamHI and XhoI restriction sites, which additionally encoded a 6$\times$His epitope on the N terminus. The resultant plasmid was transformed into *E. coli* Rosetta(DE3) (also a kind gift from Yuxin Mao). Expression was induced by addition of 0.25 mM IPTG (isopropyl-β-$_D$-thiogalactopyranoside) to a 500-ml culture of bacteria at an optical density at 600 nm (OD$_{600}$) of 0.6. The bacteria were cultured overnight (approximately 16 h) at 15°C and then centrifuged at 5,800 $\times$ g at 4°C for 30 min and resuspended in collection buffer, consisting of 20 mM Tris-HCl, pH 8.8, 500 mM NaCl, and 10 mM 2-mercaptoethanol. The bacteria were lysed by sonication, and the lysate was clarified by centrifugation at 24,500 $\times$ g at 4°C for 1 h. Proteins from the resulting supernatant were bound to equilibrated HisPur Ni-nitrilotriacetic acid (NTA) resin (Thermo-Fisher Scientific) for 1.25 h at 4°C. The resin was washed extensively with collection buffer, and then protein was eluted in collection buffer with 400 mM imidazole. The protein was desalted and concentrated using a Centriprep centrifugal filter (10 kDa; EMD Millipore, Burlington, MA). The resultant protein was snap-frozen in liquid nitrogen, stored at −80°C, and used in nuclease activity assays.

Nuclease activity was assessed as previously described for HHV-1 (34). Briefly, 25-μl reaction mixtures containing 20 mM Tris-HCl, pH 7.6, 10 mM NaCl, 1 mM MgCl$_2$, 400 ng pET-20b(+) plasmid (EMD Millipore), 370 nM pUL15-C, and 0 to 10,000 μM raltegravir were incubated for 1 h at 37°C. Undigested and EcoRI-digested pET-20b(+) plasmids were included as negative and positive controls. Nuclease activity was terminated by addition of EDTA to a final concentration of 40 mM. Samples were resolved by gel electrophoresis on a 1% agarose gel containing GelRed nucleic acid gel stain (VWR). The percentage of plasmid that was nicked or linearized was determined using ImageJ (version 1.51k).

FeHV-1 ICP8 expression, purification, and activity assay. FeHV-1 ICP8 was expressed using the Bac-to-Bac baculovirus expression system (Invitrogen, Carlsbad, CA) and purified as described for HHV-1 (50). The full-length FeHV-1 strain FH2CS ICP8 gene was amplified. A 6$\times$His tag was added to the ICP8 N terminus, flanked by XbaI and EcoRI restriction enzyme sites (nucleotide sequence, TCTAGA<u>ATG</u>GAG TTCCATCATCATCATCATCATGAATTC-FeHV-1 FH2CS ICP8; the start codon is underlined), and a KpnI site was added after the C terminus. A pFastBac1 vector encoding canine parvovirus VP2 was digested with XbaI and KpnI to remove the gene, and the plasmid backbone was then purified. The modified ICP8 fragment was then cloned into this pFastBac1 vector between the XbaI and KpnI sites (pFastBac1-FH2CS ICP8). Recombinant bacmids were generated by transforming chemically competent *E. coli* DH10Bac cells (Invitrogen) with pFastBac1-FH2CS ICP8, according to the manufacturer's instructions. Sf9 insect cells were transfected with recombinant bacmids using TransIT-Insect transfection reagent (Mirus Bio, Madison, WI) according to the manufacturer's protocol. The supernatant from the transfected cells was collected and designated the P1 stock. This was used to infect new Sf9 cells to generate a P2 stock. The

TABLE 2 Primer sequences used for qRT-PCR in this study

Gene	Viral gene classification[a]	Viral protein	Primer sequence[b] (5'–3')	
			Forward	Reverse
RL2	IE	ICP0	GTGTGACATCGCTCATCCAC	GGATCCCAATCGAGATACTCC
UL54	IE	ICP27	TCGTTACGTCCTCCAATTCC	AGCCGCTCCAAACATATCAC
UL23	E	Thymidine kinase	CAATCCAATCGAGAGTGGTG	GACATCGGTACGTGGTTCG
UL29	E	ICP8	AGACCAAACGACAACGAACC	CCTTGCTGCTCCATATCACC
UL10	L	Glycoprotein M	CGCCAGCCTTCTCAATTATC	CGCAACCTCGACGTAAAATC
UL19	L	Major capsid protein	GAACTGCCGATCAACTCCTC	CCCATACTATGCCCACCATC
UL20	L	UL20	CGTCTCATCATCGGATTCTC	CCACGGCGTCACATATAGC
UL24	L	UL24	CAATCCAATCGAGAGTGGTG	GACATCGGTACGTGGTTCG
UL27	L	Glycoprotein B	CAGACTGGAACCCTGGAGAC	ATCTACCGTGCGATTGGAAC
UL38	L	Minor capsid protein	CTATATGCGCCTCGGTATCC	CACGGGAACTTCAACACCTC
UL44	L	Glycoprotein C	TCTTGACGGGAAGCCAATAG	TGTCGGAATAGCCAACACAG
US6	L	Glycoprotein D	CAGACGATGAACTGGGTTTG	CAACATGGCGTTGGAGATAG
US7	L	Glycoprotein I	TAATGCTTTCCGGTCCTGTC	TACCCGCAGTGCGTAGATTC
RPL17	NA	NA	AAGAACACACGGGAAACTGC	CTGGGCACACCTACCAACTC

[a]IE, immediate early gene; E, early gene; L, late gene; NA, not applicable.
[b]All viral sequences were designed based on the C-27 FeHV-1 strain.

P2 stock was then used to infect High Five (*Trichoplusia ni*) cells (Boyce Thompson Institute; clone BTI-TN-551-4) for the expression of ICP8.

ICP8 was purified as described for HHV-1 ICP8 (50). Briefly, cells were collected by centrifugation at $200 \times g$ for 15 min. The resultant cell pellet was resuspended in lysis buffer (20 mM Tris-HCl, pH 7.5, 300 mM NaCl, 20% glycerol, and 0.5% NP-40), and the cells were incubated on ice for 30 min to allow lysis. The cell debris was pelleted at $12,000 \times g$ at 4°C for 15 min. Proteins from the resulting supernatant were bound to equilibrated HisPur Ni-NTA resin (Thermo-Fisher Scientific) at RT for 1 h. The bound protein was washed extensively with wash buffer consisting of 20 mM Tris-HCl, pH 7.5, 300 mM NaCl, 5% glycerol, 20 mM imidazole, and 0.1% NP-40, adjusted to pH 7.4. The protein was eluted with wash buffer containing 400 mM imidazole, buffer exchanged into water on a PD Minitrap G-25 column (GE Healthcare), rebound to beads as described above, and washed with wash buffer containing increasing concentrations of imidazole (0 to 400 mM). Fractions containing ICP8, as determined by Coomassie gels, were combined and buffer exchanged on an Amicon Ultra-15 centrifugal filter (50 kDa) unit (EMD Millipore) into ICP8 storage buffer consisting of 50 mM Tris-HCl, pH 7.5, 150 mM NaCl, 1 mM EDTA, and 1 mM dithiothreitol (DTT) adjusted to pH 7.4.

Single-stranded-DNA binding capacity was assessed similarly to a previously described protocol (67). Reaction mixtures (10 μl) containing 20 mM Tris-HCl, pH 7.5, 4% glycerol, 0.1 mg/ml bovine serum albumin (BSA), 0.5 mM DTT, 5 mM MgCl$_2$, and 100 nM 5' Cy3-labeled 50-nucleotide ssDNA probe (5' Cy3, TGCGGATGGCTTAGAGCTTAATTGCTGAATCTGGTGCTGTAGCTCAACAT; Sigma-Aldrich) were incubated with 200 or 500 nM FeHV-1 ICP8 and increasing concentrations of raltegravir or volume-matched amounts of DMSO for 1 h at 37°C. Reactions were terminated by addition of 2 μl of 6× loading buffer (187.5 mM Tris-HCl, pH 6.8, 40% glycerol, 0.01% bromophenol blue). Mixtures were separated on 5% nondenaturing PAGE gels, and Cy3 fluorescent signals were visualized using a Bio-Rad ChemiDoc MP imaging system. The percentage of probe that was shifted was determined using ImageJ (version 1.51k) and normalized to untreated controls.

DNA polymerase-pausing assay. Similar to previous studies (44), confluent CRFK cells were infected with FeHV-1 at an MOI of 2 for 12 h and treated at the time of infection with 100 μg/ml PAA to inhibit DNA elongation by the viral DNA polymerase. The inoculum and PAA were removed to release the cells from PAA block and replaced with cell line medium containing no drugs, 100 μg/ml PAA, 100 μg/ml PAA with 50 μg/ml CHX, 50 μg/ml CHX, 500 μM raltegravir, or 500 μM raltegravir with 50 μg/ml CHX. The cells were cultured for an additional 16 h, at which point they were collected and gDNA was isolated using a Qiagen blood and tissue kit. Relative genome quantification was determined using SYBR green-based qPCR targeting viral ICP4 and the feline ribosomal protein L17 housekeeping gene (*RPL17*) (Table 2), using an Applied Biosystems 7500 Fast Real Time PCR instrument (Applied Biosystems, Carlsbad, CA) in triplicate, and expressed relative to DMSO-treated samples using the comparative threshold cycle (C_t) method ($2^{-\Delta\Delta CT}$).

Analysis of viral gene expression. To evaluate viral gene expression during a single-step infection, confluent FCEC cultures were infected with FeHV-1 at an MOI of 10 and treated at the time of infection with DMSO, 500 μM raltegravir, 12.5 μg/ml PAA, or 200 μg/ml PAA for 6 h. The cells were lysed with a QIAshredder column (Qiagen), the lysates were passed through a gDNA eliminator column to remove gDNA, and RNA was then isolated using an RNeasy Plus minikit (Qiagen). cDNA was synthesized using Moloney murine leukemia virus (MMLV) reverse transcriptase. Primers were designed using Primer3 (version 0.4.0) (68), based on the FeHV-1 C-27 reference strain or the feline reference genome in the NCBI GenBank database (Table 2). SYBR green-based qRT-PCR assays were performed using an Applied Biosystems 7500 Fast Real Time PCR instrument (Applied Biosystems, Carlsbad, CA), and all samples were run in triplicate. The $2^{-\Delta\Delta Ct}$ method was used to calculate the fold change relative to DMSO- or DMEM-treated samples.

Flow cytometric evaluation of gD expression. Flow cytometry was used to determine the kinetics of gD protein expression in drug-treated cells. Confluent FCECs were infected with FeHV-1–gD–DsRed (48) at an MOI of 3 or mock infected and treated at the time of infection with DMSO, 500 μM raltegravir, or 12.5 μg/ml PAA. Cells were collected at 0, 6, 12, 18, and 24 hpi via trypsinization and rinsed once with phosphate-buffered saline (PBS). After rinsing, 20,000 live cells were analyzed on a Gallios flow cytometer controlled by Kaluza for Gallios software (Beckman Coulter, Indianapolis, IN). Data analysis was conducted using FlowJo version 10.4.1 (FlowJo LLC, Ashland, OR).

Statistical analysis. Data were statistically evaluated using GraphPad Prism version 6.04 for Windows and are expressed as means and standard deviations. Student t tests were used to compare 2 groups, and one-way ANOVA with a Tukey HSD *post hoc* test was used where 3 or more groups were compared. Fisher's exact test was used to analyze the results of electron microscopy. All experiments, with the exception of electron microscopy, were performed at least three times. A P value of ≤ 0.05 was considered significant.

Accession number(s). All the reads from the experiments have been submitted to the NCBI as Sequence Read Archive (SRA) data sets under SRA study accession no. SRP148532.

ACKNOWLEDGMENTS

REFERENCES

1. Davison AJ, Eberle R, Ehlers B, Hayward GS, McGeoch DJ, Minson AC, Pellett PE, Roizman B, Studdert MJ, Thiry E. 2009. The order Herpesvirales. Arch Virol 154:171–177. https://doi.org/10.1007/s00705-008-0278-4.

2. Looker KJ, Magaret AS, May MT, Turner KME, Vickerman P, Gottlieb SL, Newman LM. 2015. Global and regional estimates of prevalent and incident herpes simplex virus type 1 infections in 2012. PLoS One 10:e0140765. https://doi.org/10.1371/journal.pone.0140765.

3. Rowe AM, St Leger AJ, Jeon S, Dhaliwal DK, Knickelbein JE, Hendricks RL. 2013. Herpes keratitis. Prog Retin Eye Res 32:88–101. https://doi.org/10.1016/j.preteyeres.2012.08.002.

4. Austin A, Lietman T, Rose-Nussbaumer J. 2017. Update on the management of infectious keratitis. Ophthalmology 124:1678–1689. https://doi.org/10.1016/j.ophtha.2017.05.012.

5. Andrei G, Snoeck R. 2013. Herpes simplex virus drug-resistance. Curr Opin Infect Dis 26:551–560. https://doi.org/10.1097/QCO.0000000000000015.

6. Tsatsos M, MacGregor C, Athanasiadis I, Moschos MM, Hossain P, Anderson D. 2016. Herpes simplex virus keratitis: an update of the pathogenesis and current treatment with oral and topical antiviral agents. Clin Exp Ophthalmol 44:824–837. https://doi.org/10.1111/ceo.12785.

7. Piret J, Boivin G. 2016. Antiviral resistance in herpes simplex virus and varicella-zoster virus infections. Curr Opin Infect Dis 29:654–662. https://doi.org/10.1097/QCO.0000000000000288.

8. Azher TN, Yin X-T, Tajfirouz D, Huang AJ, Stuart PM. 2017. Herpes simplex keratitis: challenges in diagnosis and clinical management. Clin Ophthalmol 11:185–191. https://doi.org/10.2147/OPTH.S80475.

9. Al-Dujaili LJ, Clerkin PP, Clement C, McFerrin HE, Bhattacharjee PS, Varnell ED, Kaufman HE, Hill JM. 2011. Ocular herpes simplex virus: how are latency, reactivation, recurrent disease and therapy interrelated? Future Microbiol 6:877–907. https://doi.org/10.2217/fmb.11.73.

10. Law GL, Tisoncik-Go J, Korth MJ, Katze MG. 2013. Drug repurposing: a better approach for infectious disease drug discovery? Curr Opin Immunol 25:588–592. https://doi.org/10.1016/j.coi.2013.08.004.

11. Mounce BC, Cesaro T, Moratorio G, Hooikaas PJ, Yakovleva A, Werneke SW, Smith EC, Poirier EZ, Simon-Loriere E, Prot M, Tamietti C, Vitry S, Volle R, Khou C, Frenkiel M-P, Sakuntabhai A, Delpeyroux F, Pardigon N, Flamand M, Barba-Spaeth G, Lafon M, Denison MR, Albert ML, Vignuzzi M. 2016. Inhibition of polyamine biosynthesis is a broad-spectrum strategy against RNA viruses. J Virol 90:9683–9692. https://doi.org/10.1128/JVI.01347-16.

12. Johansen LM, Brannan JM, Delos SE, Shoemaker CJ, Stossel A, Lear C, Hoffstrom BG, Dewald LE, Schornberg KL, Scully C, Lehár J, Hensley LE, White JM, Olinger GG. 2013. FDA-approved selective estrogen receptor modulators inhibit Ebola virus infection. Sci Transl Med 5:190ra79. https://doi.org/10.1126/scitranslmed.3005471.

13. Dyall J, Coleman CM, Hart BJ, Venkataraman T, Holbrook MR, Kindrachuk J, Johnson RF, Olinger GG, Jahrling PB, Laidlaw M, Johansen LM, Lear-Rooney CM, Glass PJ, Hensley LE, Frieman MB. 2014. Repurposing of clinically developed drugs for treatment of Middle East respiratory syndrome coronavirus infection. Antimicrob Agents Chemother 58:4885–4893. https://doi.org/10.1128/AAC.03036-14.

14. Albulescu IC, van Hoolwerff M, Wolters LA, Bottaro E, Nastruzzi C, Yang SC, Tsay S-C, Hwu JR, Snijder EJ, van Hemert MJ. 2015. Suramin inhibits chikungunya virus replication through multiple mechanisms. Antiviral Res 121:39–46. https://doi.org/10.1016/j.antiviral.2015.06.013.

15. Summa V, Petrocchi A, Bonelli F, Crescenzi B, Donghi M, Ferrara M, Fiore F, Gardelli C, Gonzalez Paz O, Hazuda DJ, Jones P, Kinzel O, Laufer R, Monteagudo E, Muraglia E, Nizi E, Orvieto F, Pace P, Pescatore G, Scarpelli R, Stillmock K, Witmer MV, Rowley M. 2008. Discovery of raltegravir, a potent, selective orally bioavailable HIV-integrase inhibitor for the treatment of HIV-AIDS infection. J Med Chem 51:5843–5855. https://doi.org/10.1021/jm800245z.

16. Mouscadet JF, Tchertanov L. 2009. Raltegravir: molecular basis of its mechanism of action. Eur J Med Res 14(Suppl 3):S5–S16. https://doi.org/10.1186/2047-783X-14-S3-5.

17. McColl DJ, Chen X. 2010. Strand transfer inhibitors of HIV-1 integrase: bringing IN a new era of antiretroviral therapy. Antiviral Res 85:101–118. https://doi.org/10.1016/j.antiviral.2009.11.004.

18. Nadal M, Mas PJ, Mas PJ, Blanco AG, Arnan C, Solà M, Hart DJ, Coll M. 2010. Structure and inhibition of herpesvirus DNA packaging terminase nuclease domain. Proc Natl Acad Sci U S A 107:16078–16083. https://doi.org/10.1073/pnas.1007144107.

19. Bogner E. 2002. Human cytomegalovirus terminase as a target for antiviral chemotherapy. Rev Med Virol 12:115–127. https://doi.org/10.1002/rmv.344.

20. Bowman LJ, Melaragno JI, Brennan DC. 2017. Letermovir for the management of cytomegalovirus infection. Expert Opin Investig Drugs 26:235–241. https://doi.org/10.1080/13543784.2017.1274733.

21. Zhou B, Yang K, Wills E, Tang L, Baines JD. 2014. A mutation in the DNA polymerase accessory factor of herpes simplex virus 1 restores viral DNA replication in the presence of raltegravir. J Virol 88:11121–11129. https://doi.org/10.1128/JVI.01540-14.

22. Maes R. 2012. Felid herpesvirus type 1 infection in cats: a natural host

model for alphaherpesvirus pathogenesis. ISRN Vet Sci 2012:495830. https://doi.org/10.5402/2012/495830.

23. Pennington M, Ledbetter E, Van de Walle G. 2017. New paradigms for the study of ocular alphaherpesvirus infections: insights into the use of non-traditional host model systems. Viruses 9:E349. https://doi.org/10.3390/v9110349.

24. Gaskell R, Dawson S, Radford A, Thiry E. 2007. Feline herpesvirus. Vet Res 38:337–354. https://doi.org/10.1051/vetres:2006063.

25. Thomasy SM, Maggs DJ. 2016. A review of antiviral drugs and other compounds with activity against feline herpesvirus type 1. Vet Ophthalmol 19:119–130. https://doi.org/10.1111/vop.12375.

26. Pennington MR, Fort MW, Ledbetter EC, Van de Walle GR. 2016. A novel corneal explant model system to evaluate antiviral drugs against feline herpesvirus type 1 (FHV-1). J Gen Virol 97:1414–1425. https://doi.org/10.1099/jgv.0.000451.

27. Vaz PK, Job N, Horsington J, Ficorilli N, Studdert MJ, Hartley CA, Gilkerson JR, Browning GF, Devlin JM. 2016. Low genetic diversity among historical and contemporary clinical isolates of felid herpesvirus 1. BMC Genomics 17:704. https://doi.org/10.1186/s12864-016-3050-2.

28. Kolb AW, Lewin AC, Moeller Trane R, McLellan GJ, Brandt CR. 2017. Phylogenetic and recombination analysis of the herpesvirus genus varicellovirus. BMC Genomics 18:887. https://doi.org/10.1186/s12864-017-4283-4.

29. Lewin AC, Kolb AW, McLellan GJ, Bentley E, Bernard KA, Newbury SP, Brandt CR. 2018. Genomic, recombinational and phylogenetic characterization of global feline herpesvirus 1 isolates. Virology 518:385–397. https://doi.org/10.1016/j.virol.2018.03.018.

30. Sauerbrei A, Bohn K, Heim A, Hofmann J, Weißbrich B, Schnitzler P, Hoffmann D, Zell R, Jahn G, Wutzler P, Hamprecht K. 2011. Novel resistance-associated mutations of thymidine kinase and DNA polymerase genes of herpes simplex virus type 1 and type 2. Antivir Ther 16:1297–1308. https://doi.org/10.3851/IMP1870.

31. Frobert E, Burrel S, Ducastelle-Lepretre S, Billaud G, Ader F, Casalegno JS, Nave V, Boutolleau D, Michallet M, Lina B, Morfin F. 2014. Resistance of herpes simplex viruses to acyclovir: an update from a ten-year survey in France. Antiviral Res 111:36–41. https://doi.org/10.1016/j.antiviral.2014.08.013.

32. Schmidt S, Bohn-Wippert K, Schlattmann P, Zell R, Sauerbrei A. 2015. Sequence analysis of herpes simplex virus 1 thymidine kinase and DNA polymerase genes from over 300 clinical isolates from 1973 to 2014 finds novel mutations that may be relevant for development of antiviral resistance. Antimicrob Agents Chemother 59:4938–4945. https://doi.org/10.1128/AAC.00977-15.

33. Goldner T, Hewlett G, Ettischer N, Ruebsamen-Schaeff H, Zimmermann H, Lischka P. 2011. The novel anticytomegalovirus compound AIC246 (Letermovir) inhibits human cytomegalovirus replication through a specific antiviral mechanism that involves the viral terminase. J Virol 85:10884–10893. https://doi.org/10.1128/JVI.05265-11.

34. Selvarajan Sigamani S, Zhao H, Kamau YN, Baines JD, Tang L. 2013. The structure of the herpes simplex virus DNA-packaging terminase pUL15 nuclease domain suggests an evolutionary lineage among eukaryotic and prokaryotic viruses. J Virol 87:7140–7148. https://doi.org/10.1128/JVI.00311-13.

35. Yan Z, Bryant KF, Gregory SM, Angelova M, Dreyfus DH, Zhao XZ, Coen DM, Burke TR, Knipe DM. 2014. HIV integrase inhibitors block replication of alpha-, beta-, and gammaherpesviruses. mBio 5:e01318-14. https://doi.org/10.1128/mBio.01318-14.

36. Ruyechan WT, Weir AC. 1984. Interaction with nucleic acids and stimulation of the viral DNA polymerase by the herpes simplex virus type 1 major DNA-binding protein. J Virol 52:727–733.

37. Leinbach SS, Heath LS. 1989. Characterization of the single-stranded DNA-binding domain of the herpes simplex virus protein ICP8. Biochim Biophys Acta 1008:281–286. https://doi.org/10.1016/0167-4781(89)90017-1.

38. Nimonkar AV, Boehmer PE. 2002. In vitro strand exchange promoted by the herpes simplex virus type-1 single strand DNA-binding protein (ICP8) and DNA helicase-primase. J Biol Chem 277:15182–15189. https://doi.org/10.1074/jbc.M109988200.

39. Reuven NB, Staire AE, Myers RS, Weller SK. 2003. The herpes simplex virus type 1 alkaline nuclease and single-stranded DNA binding protein mediate strand exchange in vitro. J Virol 77:7425–7433. https://doi.org/10.1128/JVI.77.13.7425-7433.2003.

40. Reuven NB, Willcox S, Griffith JD, Weller SK. 2004. Catalysis of strand exchange by the HSV-1 UL12 and ICP8 proteins: potent ICP8 recombinase activity is revealed upon resection of dsDNA substrate by nuclease. J Mol Biol 342:57–71. https://doi.org/10.1016/j.jmb.2004.07.012.

41. Gao M, Knipe DM. 1991. Potential role for herpes simplex virus ICP8 DNA replication protein in stimulation of late gene expression. J Virol 65:2666–2675.

42. Chen Y, Knipe D. 1996. A dominant mutant form of the herpes simplex virus ICP8 protein decreases viral late gene transcription. Virology 221:281–290. https://doi.org/10.1006/viro.1996.0377.

43. Wilkinson D, Weller S. 2003. The role of DNA recombination in herpes simplex virus DNA replication. IUBMB Life 55:451–458. https://doi.org/10.1080/15216540310001612237.

44. Schang LM, Rosenberg A, Schaffer PA. 2000. Roscovitine, a specific inhibitor of cellular cyclin-dependent kinases, inhibits herpes simplex virus DNA synthesis in the presence of viral early proteins. J Virol 74:2107–2120. https://doi.org/10.1128/JVI.74.5.2107-2120.2000.

45. Becker Y, Asher Y, Cohen Y, Weinberg-Zahlering E, Shlomai J. 1977. Phosphonoacetic acid-resistant mutants of herpes simplex virus: effect of phosphonoacetic acid on virus replication and in vitro deoxyribonucleic acid synthesis in isolated nuclei. 11:919–922.

46. Gruffat H, Marchione R, Manet E. 2016. Herpesvirus late gene expression: a viral-specific pre-initiation complex is key. Front Microbiol 7:869. https://doi.org/10.3389/fmicb.2016.00869.

47. Pennington MR, Grenier JK, Van de Walle GR. 2018. Transcriptome profiling of alphaherpesvirus-infected cells treated with the HIV-integrase inhibitor raltegravir reveals profound and specific alterations in host transcription. J Gen Virol 99:1115–1128. https://doi.org/10.1099/jgv.0.001090.

48. Pennington MR, Van de Walle GR. 2017. Electric cell-substrate impedance sensing to monitor viral growth and study cellular responses to infection with alphaherpesviruses in real time. mSphere 2:e00039-17. https://doi.org/10.1128/mSphere.00039-17.

49. Honess RW, Watson DH. 1977. Herpes simplex virus resistance and sensitivity to phosphonoacetic acid. J Virol 21:584–600.

50. Bryant KF, Yan Z, Dreyfus DH, Knipe DM. 2012. Identification of a divalent metal cation bindings site in herpes simplex virus 1 (HSV-1) ICP8 required for HSV replication. J Virol 86:6825–6834. https://doi.org/10.1128/JVI.00374-12.

51. Leinbach SS, Casto JF. 1983. Identification and characterization of deoxyribonucleoprotein complexes containing the major DNA-binding protein of herpes simplex virus type 1. Virology 131:274–286. https://doi.org/10.1016/0042-6822(83)90496-8.

52. Boehmer PE, Dodson MS, Lehman IR. 1993. The herpes simplex virus type-1 origin binding protein. DNA helicase activity. J Biol Chem 268:1220–1225.

53. Makhov AM, Lee SSK, Lehman IR, Griffith JD. 2003. Origin-specific unwinding of herpes simplex virus 1 DNA by the viral UL9 and ICP8 proteins: visualization of a specific preunwinding complex. Proc Natl Acad Sci U S A 100:898–903. https://doi.org/10.1073/pnas.0237171100.

54. Arana ME, Haq B, Tanguy Le Gac N, Boehmer PE. 2001. Modulation of the herpes simplex virus type-1 UL9 DNA helicase by its cognate single-strand DNA-binding protein, ICP8. J Biol Chem 276:6840–6845. https://doi.org/10.1074/jbc.M007219200.

55. Arsenakis M, Campadelli-Fiume G, Roizman B. 1988. Regulation of glycoprotein D synthesis: does alpha 4, the major regulatory protein of herpes simplex virus 1, regulate late genes both positively and negatively? J Virol 62:148–158.

56. Nimonkar AV, Boehmer PE. 2003. The herpes simplex virus type-1 single-strand DNA-binding protein (ICP8) promotes strand invasion. J Biol Chem 278:9678–9682. https://doi.org/10.1074/jbc.M212555200.

57. Reuven NB, Weller SK. 2005. Herpes simplex virus type 1 single-strand DNA binding protein ICP8 enhances the nuclease activity of the UL12 alkaline nuclease by increasing its processivity. J Virol 79:9356–9358. https://doi.org/10.1128/JVI.79.14.9356-9358.2005.

58. Weller SK, Coen DM. 2012. Herpes simplex viruses: mechanisms of DNA replication. Cold Spring Harb Perspect Biol 4:a013011. https://doi.org/10.1101/cshperspect.a013011.

59. Ireland PJ, Tavis JE, D'Erasmo MP, Hirsch DR, Murelli RP, Cadiz MM, Patel BS, Gupta AK, Edwards TC, Korom M, Moran EA, Morrison LA. 2016. Synthetic α-hydroxytropolones inhibit replication of wild-type and acyclovir-resistant herpes simplex viruses. Antimicrob Agents Chemother 60:2140–2149. https://doi.org/10.1128/AAC.02675-15.

60. Masaoka T, Zhao H, Hirsch DR, D'Erasmo MP, Meck C, Varnado B, Gupta A, Meyers MJ, Baines J, Beutler JA, Murelli RP, Tang L, Le Grice SFJ. 2016. Characterization of the C-terminal nuclease domain of herpes simplex virus pUL15 as a target of nucleotidyltransferase inhibitors. Biochemistry 55:809–819. https://doi.org/10.1021/acs.biochem.5b01254.

61. Dehghanpir SD, Birkenheuer CH, Yang K, Murelli RP, Morrison LA, Le Grice SFJ, Baines JD. 2018. Broad anti-herpesviral activity of α-hydroxytropolones. Vet Microbiol 214:125–131. https://doi.org/10.1016/j.vetmic.2017.12.016.

62. Sandmeyer LS, Keller CB, Bienzle D. 2005. Culture of feline corneal epithelial cells and infection with feline herpesvirus-1 as an investigative tool. Am J Vet Res 66:205–209. https://doi.org/10.2460/ajvr.2005.66.205.

63. Walton TE, Gillespie JH. 1970. Feline viruses. VII. Immunity to the feline herpesvirus in kittens inoculated experimentally by the aerosol method. Cornell Vet 60:232–239.

64. Tai SHS, Niikura M, Cheng HH, Kruger JM, Wise AG, Maes RK. 2010. Complete genomic sequence and an infectious BAC clone of feline herpesvirus-1 (FHV-1). Virology 401:215–227. https://doi.org/10.1016/j.virol.2010.02.021.

65. Pizzurro F, Mangone I, Zaccaria G, De Luca E, Malatesta D, Innocenti M, Carmine I, Cito F, Marcacci M, Di Sabatino D, Lorusso A. 2016. Whole-genome sequence of a suid herpesvirus-1 strain isolated from the brain of a hunting dog in Italy. Genome Announc 4:e01333-16. https://doi.org/10.1128/genomeA.01333-16.

66. Le Sage V, Jung M, Alter JD, Wills EG, Johnston SM, Kawaguchi Y, Baines JD, Banfield BW. 2013. The herpes simplex virus 2 UL21 protein is essential for virus propagation. J Virol 87:5904–5915. https://doi.org/10.1128/JVI.03489-12.

67. Darwish AS, Grady LM, Bai P, Weller SK. 2015. ICP8 filament formation is essential for replication compartment formation during herpes simplex virus infection. J Virol 90:2561–2570. https://doi.org/10.1128/JVI.02854-15.

68. Untergasser A, Cutcutache I, Koressaar T, Ye J, Faircloth BC, Remm M, Rozen SG. 2012. Primer3; new capabilities and interfaces. Nucleic Acids Res 40:e115. https://doi.org/10.1093/nar/gks596.